

## Specific features of microhardness and thermodynamic stability of the $\text{Cd}_{1-x}\text{Mn}_x\text{Te}$ solid solutions

K.S. Dremluzhenko<sup>1</sup>, I.M. Yuriychuk<sup>2</sup>, Z.I. Zakharuk<sup>2</sup>, V.G. Deibuk<sup>2\*</sup>

<sup>1</sup>V. Lashkaryov Institute of Semiconductor Physics, 03680 Kyiv, Ukraine

<sup>2</sup>Yuriy Fedkovych Chernivtsi National University, 58012 Chernivtsi, Ukraine

\*Corresponding author e-mail: v.deibuk@chnu.edu.ua

**Abstract.** The features of fusion and growth of  $\text{Cd}_{1-x}\text{Mn}_x\text{Te}$  ( $0.02 \leq x \leq 0.55$ ) solid solution crystals as well as the dependence of their microhardness on the composition have been studied. Local maxima of the microhardness at  $x = 0.14$  and  $0.46$  have been experimentally found. Thermodynamics of  $\text{Cd}_{1-x}\text{Mn}_x\text{Te}$  formation in the delta-lattice parameter model has been considered, and the phase diagram of spinodal decomposition in these solid solutions has been found. The empirical pseudopotential method was used to analyze the distribution of the valence charge density during formation of the  $\text{Cd}_{1-x}\text{Mn}_x\text{Te}$  solid solution and its effect on the rearrangement of chemical bonds. It has been shown that the stability of the solid solutions is defined not only by the difference in the lattice constants of the CdTe and MnTe binary compounds but also by the charge exchange between bonds with the different degree of ionicity and the change in the nature of chemical bonds.

**Keywords:** microhardness, semiconductor, solid solution, thermodynamic stability, spinodal decomposition.

<https://doi.org/10.15407/spqeo25.03.282>

PACS 62.20.-x

Manuscript received 17.03.22; revised version received 02.08.22; accepted for publication 21.09.22; published online 06.10.22.

### 1. Introduction

The study of  $\text{Cd}_{1-x}\text{Mn}_x\text{Te}$  crystals has attracted considerable interest in recent years due to the prospects for their use in electronics as light filters, Faraday cells in optical isolators, the base material for manufacturing radiation sensors, *etc* [1–3]. For these purposes, homogeneous and structurally perfect crystals are needed. However, the growth of high-quality  $\text{Cd}_{1-x}\text{Mn}_x\text{Te}$  material is difficult because of the features inherent to physical-and-chemical properties of these solid solutions.

Data on the nature of physical-and-chemical interaction in the CdTe–MnTe–Te system are currently available [4]. With account of known parameters of the phase equilibrium in the system, integral values of the Gibbs energy, enthalpy and formation entropy of  $\text{MnTe}_2$ , MnTe can be calculated. XRD was used to triangulate the CdTe–MnTe–Te system at 643 K [4, 5]. Particular attention was drawn to the CdTe–MnTe cross section, since solid solutions on the basis of these binary compounds can be formed: from the CdTe side up to 77 mol.% of MnTe [6, 7] and up to 71.4 mol.% of MnTe according to [8], as well as from the MnTe side ( $\alpha$ -modification) up to 0.3 mol.% of CdTe [8]. The presence of two compounds ( $\text{MnTe}_2$  and MnTe) in the Mn–Te system [9] with four high-temperature

polymorphic transformations complicates the possibility of obtaining a single-phase, homogeneous, structurally perfect material.

The aim of this work was to study the features of the  $\text{Cd}_{1-x}\text{Mn}_x\text{Te}$  solid solution microhardness. In addition, a series of experiments was carried out to clarify the effect of synthesis time on the distribution of the manganese over the volume and length of the ingot, as well as quality of the obtained ingots. The lattice constant and microhardness of the obtained crystalline solid solutions were measured, and also the thermodynamic stability and nature of the chemical bond in this material were studied.

### 2. Experimental

The  $\text{Cd}_{1-x}\text{Mn}_x\text{Te}$  solid solution alloys were obtained using direct alloying of stoichiometric quantities of initial components with the purity class not lower than N6. The synthesis of the  $\text{Cd}_{1-x}\text{Mn}_x\text{Te}$  alloys is sometimes accompanied by interaction of the charge with the material of the graphitized silica container. This especially often occurs at high concentrations of manganese. The main factor that causes interaction of the charge with the material of container is the presence of oxides, which are introduced with the source of manganese. The latter is a chemically active component and is highly oxidized

in air. In this case, the synthesis of alloys in a hydrogen atmosphere is not a solution, since hydrogen does not reduce manganese oxides. Therefore, the source of Mn was constantly stored in vacuum, and the fusion container was covered with a dense layer of pyrolytic graphite.

The crystals were grown from the alloys by the Bridgman method (temperature gradient at the crystallization was 10...15 K/cm, growth rate – 2 mm/h). We used two types of setups. In the first case, being fixed on the rod ampoule the material was located in the temperature field of the fixed heater. In this setup, it is impossible to get rid of vibration, microswinging, and other disturbances in the smoothness of the ampoule movement, which has a bad effect on the structure of the grown crystal. In the second case, the heater moved relatively to the fixed ampoule. To stabilize the movement, the weight of the heater was balanced by two massive counterweights. To prevent rocking, the heater was connected by a system of rollers to a fixed rail. In this case, the violation of the smoothness of the movement was eliminated due to the high mass of the heater and the damping effect of the rollers. Quality of the resulting monocrystalline blocks depends on the uniformity of the components distribution in the solid solution as well as duration of the synthesis and growth. To determine the optimal parameters of the technological process, we carried out experiments to study the effect of synthesis and growth time on the distribution of the manganese over the volume of ingot as well as on the structure of obtained ingots. Technological modes were corrected being based on the results of studying the distribution of manganese in the  $\text{Cd}_{1-x}\text{Mn}_x\text{Te}$  by measuring the microhardness and using the radioisotope method.

The study of microhardness in the prepared  $\text{Cd}_{1-x}\text{Mn}_x\text{Te}$  crystalline samples was carried out using the PMT-3 device. Since the surface state affects the results of microhardness measurements, the damaged surface layer was removed by mechanical grinding, polishing and treatment in the bromine-methanol etchant. At least 10 pricks were made on each sample and the average value was determined. In this case, the error in determining the microhardness did not exceed 2-3%. As a reference material, the NaCl single crystal was used. The microhardness of  $\text{Cd}_{1-x}\text{Mn}_x\text{Te}$  solid solutions at low loads on the indenter (5...20 g) monotonically increased with increasing load, and within the range 20...100 g practically did not depend on the value of the load. Therefore, the optimal value of the load on the indenter was 50 g. For X-ray studies, the single crystal samples were oriented along the (111) or (110) crystallographic planes. To reduce distortion of the crystal lattice by the damaged surface layer, the surface of the samples was treated in a polishing etchant after grinding with abrasive powders and polishing with diamond pastes. The structural perfection of the crystals was studied using the Berg–Barrett topographical method as well as the double-crystal spectrometer method. The lattice constant was measured using the Bond method with an accuracy

of  $5 \cdot 10^{-4} \text{ \AA}$ . The radioisotope analysis was used to study distribution of Mn in the  $\text{Cd}_{1-x}\text{Mn}_x\text{Te}$  crystals. The  $\text{MnCl}_2$  solution labeled with the radioactive isotope  $^{54}\text{Mn}$  was added to graphitized silica ampoules and the solution was dried at the temperatures of 320...330 K. Then the calculated mass of constituent components was loaded and the mixing, fusion, and crystal growth were carried out. Introduction of the above amount of radioactive manganese provided activity of the crystalline washers of 17 Bq. The resulting ingots were cut into 2...3 mm thick washers perpendicular to the growth axis. The activity of samples was measured using the UMR-1500 setup. By comparing the activity of samples and standards, the concentration of Mn in each washer was determined.

### 3. Results and discussion

We have obtained 11 samples of the  $\text{Cd}_{1-x}\text{Mn}_x\text{Te}$  crystals, the manganese content of which varied from  $x = 0.02$  to  $x = 0.55$ . The studies showed that the inhomogeneity of the manganese distribution in the volume of ingot is observed when the duration of synthesis process is less than 70 hours. X-ray measurements revealed a chaotic dependence of the lattice constant ( $a$ ) along the axis of the  $\text{Cd}_{1-x}\text{Mn}_x\text{Te}$  ingot. The inhomogeneity of manganese distribution increased with an increase in the content of manganese, since in such alloys its distribution in the melt is significantly affected by the formation and dissolution times of  $\text{MnTe}$  as the most refractory component. The crystals with the uniform distribution of the components over the ingot were obtained after a long synthesis (more than 70 hours). The lattice constant of the  $\text{Cd}_{1-x}\text{Mn}_x\text{Te}$  solid solution did not change along the ingot, its dependence on the composition was linear (Fig. 1). X-ray studies showed that the  $\text{Cd}_{1-x}\text{Mn}_x\text{Te}$  crystals up to  $x = 0.15$  have a perfect crystalline structure, and at  $x > 0.15$  a lot of crystalline twins appear, the atomic planes are curved and exact determination of the distance between them (with an accuracy of  $10^{-4} \text{ \AA}$ ) becomes difficult. Determination of the manganese distribution by using the radioisotope method in the crystals grown using the optimized technology was performed both along the length and diameter of the ingot. It was found that the distribution of manganese along the length and diameter of the ingot is almost uniform for all compositions. The deviation from the loading composition of manganese was within the experimental errors. So, we can conclude that for the  $\text{Cd}_{1-x}\text{Mn}_x\text{Te}$  solid solution the value of Mn segregation coefficient ( $k_s$ ) is close to unity.

Formation of a solid solution, as a rule, is accompanied by an increase in hardness  $H_V$ , and in the case of a continuous series of solid solutions, the compositional dependence of  $H_V$  is described by a smooth curve with a maximum [10]. In the case of limited solubility in the solid state, the microhardness of solid solution changes depending on the composition within the homogeneity region up to saturation at a given temperature, and remains constant upon transition to the two-phase region.

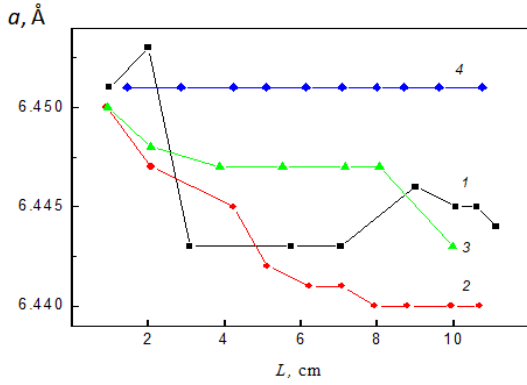


**Fig. 1.** The value of lattice constant  $a$  along the length of  $\text{Cd}_{1-x}\text{Mn}_x\text{Te}$  ingots at different synthesis durations: 18 (1), 24 (2), 30 (3), and 70 (4) hours.

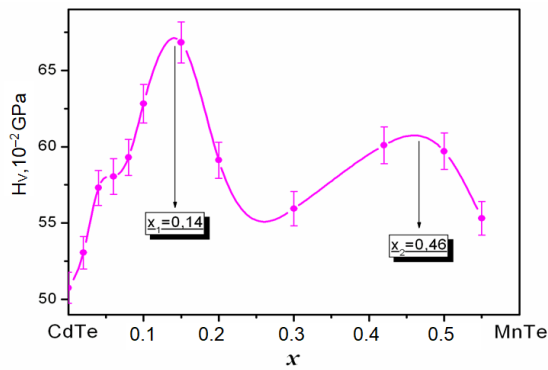


**Fig. 2.** Microhardness of the  $\text{Cd}_{1-x}\text{Mn}_x\text{Te}$  solid solutions:  $x_1$  – spinodal decomposition,  $x_2$  – redistribution of the electron density due to the local deformations.

The obtained dependence of  $H_V$  on the content of the manganese ( $x$ ) in the  $\text{Cd}_{1-x}\text{Mn}_x\text{Te}$  solid solution is shown in Fig. 2. In general, the microhardness of this solution is higher than that of CdTe. However, the dependence  $H_V(x)$  is nonmonotonic with two maxima at the manganese content  $x = 0.14$  and  $0.46$ . The explanation of the  $\text{Cd}_{1-x}\text{Mn}_x\text{Te}$  microhardness dependence on the composition  $x$  requires a more detailed study of chemical bond nature in the alloys.

Let us consider in more detail the thermodynamics of spinodal decomposition in the  $\text{Cd}_{1-x}\text{Mn}_x\text{Te}$  solid solution. At the moment, the issue of thermodynamic stability of the  $\text{A}^{\text{II}}\text{B}^{\text{VI}}$  solid solutions has not been sufficiently studied [12–14]. In addition to the analysis of the band gap and lattice constant dependences on the composition of solid solution, it is necessary to take into account the fact that most of solid solutions are unstable in a certain range of compositions. The lattice constant decreases monotonically with increasing  $x$  throughout the concentration range under study [8, 15]. The solid solution in the region of instability tends to reduce the free energy as a result of decomposition, *i.e.* phase transformation, which leads to a violation of the macroscopic homogeneity of the crystals and formation of a mixture of different composition phases.

Decomposition that proceeds without formation of new phases is called spinodal, and the corresponding curve in the state diagram, which separates the region of solid solutions compositions that are unstable even at infinitely small fluctuations of the composition, is called spinodal [16]. Disordered semiconductor alloys have a positive enthalpy of mixing, which leads to their decomposition, counteracting the stabilizing effect of internal stresses.

For thermodynamic description of the  $\text{Cd}_{1-x}\text{Mn}_x\text{Te}$  ( $\text{A}_{1-x}\text{B}_x\text{C}$ ) solid solution formation process, we consider the Gibbs free energy of mixing ( $\Delta G$ ) per mol:

$$\Delta G = \Delta H - T\Delta S, \quad (1)$$

where  $\Delta H$  is the enthalpy of mixing,  $T$  is the absolute temperature.  $\Delta S$  is the entropy of mixing, which can be written as

$$\Delta S = -RT \{ \ln x + (1-x)\ln(1-x) \}, \quad (2)$$

where  $R$  is the universal gas constant.

To describe the enthalpy of mixing, two models are often used: the model of a regular solution [16] and the model of lattice “ $\delta$ -parameter” [12]. The regular solution model describes well the thermodynamic properties of the liquid phase and has limitations for the case of the solid phase since the interaction parameters in the regular solution model depend on the composition ( $x$ ). In the model of lattice “ $\delta$ -parameter”, the enthalpy of mixing  $\Delta H$  of the  $\text{A}_{1-x}\text{B}_x\text{C}$  solid solution can be written in the form [14]:

$$\begin{aligned} \Delta H &= E(\text{alloy}) - xE(\text{BC}) - (1-x)E(\text{AC}) = \\ &= K \{ a_{\text{alloy}}^{-2.5} - xa_{\text{BC}}^{-2.5} - (1-x)a_{\text{AC}}^{-2.5} \}, \end{aligned} \quad (3)$$

where  $a_{\text{alloy}}$  is the lattice constant of the solid solution;  $E(\text{alloy})$ ,  $E(\text{AC})$ ,  $E(\text{BC})$  are the formation energies of the solid solution and compounds;  $K$  is the parameter of this model. The following parameters were chosen for the calculations [6–9]:

$$a_{\text{alloy}}(x) = 6.481(1-x) + 6.338x \text{ (\AA)}, \quad K = 1.81,$$

elastic constants:

$$C_{11}(x) = 5.3(1-x) + 4.818x \quad (10^{11}, \text{ dyn/cm}^2),$$

$$C_{12}(x) = 3.7(1-x) + 3.218x \quad (10^{11}, \text{ dyn/cm}^2).$$

The solid solution will decompose spinodally under condition that the curve of the compositional dependence of the free energy  $G(x)$  has an inflection point. The stability condition for pseudobinary alloys can be written in the form  $\partial^2 G / \partial x^2 > 0$ . The instability region is defined as the locus of points, for which the condition  $\partial^2 G / \partial x^2 = 0$  is satisfied. For a bulk solid solution, in addition to the chemical part of the free energy, it is also necessary to take into account the elastic component, which arises from the requirement of a coherent phase conjugation due to anisotropy of the crystal. The elastic strain energy  $E_s$  per unit volume can be written as follows [18]:

$$E_s = \frac{E\varepsilon^2}{1-\nu}, \quad (4)$$

$$\nu = \frac{C_{11}}{C_{11}+C_{12}}, \quad (5)$$

$$E = \frac{C_{11}+2C_{12}}{C_{11}+C_{12}}(C_{11}-C_{12}), \quad (6)$$

where  $\varepsilon$  is the elastic deformation coefficient,  $E$  is the Young modulus,  $\nu$  is the Poisson ratio. The relative deformation of crystal can be represented as

$$\varepsilon(x) = (a_{\text{alloy}}(x) - a_0) / a_0. \quad (7)$$

Thus, the total Gibbs free energy of the system per unit volume is the sum of the chemical energy  $\Delta G$  and the elastic energy  $E_s$ :

$$G_{\text{tot}} = N_v \Delta G + E'_s, \quad (8)$$

where  $N_v$  is the number of moles per unit volume of a homogeneous solid solution before decomposition. The phase diagram of  $\text{Cd}_{1-x}\text{Mn}_x\text{Te}$  solid solution spinodal decomposition calculated as the locus of points satisfying the condition  $\partial^2 G / \partial x^2 = 0$  is presented in Fig. 3. The calculated critical temperature is  $T_c = 530$  K at  $x_c = 0.48$  (see Fig. 3). The internal local deformations arising from the mixing of two components CdTe and MnTe with mismatched lattice constants lead to asymmetry of the spinodal decomposition curves. An increase in the Mn content leads to a strong deformation of the compositional dependence of the Gibbs free energy. This, in turn, affects the spinodal decomposition curve (Fig. 3). It is possible that the presence of several polymorphic modifications of MnTe and their transition from one to another also have a certain effect [9]. A decrease in the microhardness of the  $\text{Cd}_{1-x}\text{Mn}_x\text{Te}$  solid solutions at  $x \geq 0.15$  can be initiated by spinodal decomposition, which, in turn, causes continuous twinning. The change in microhardness observed near the boundaries of twinning  $\text{Cd}_{1-x}\text{Mn}_x\text{Te}$  solid solution is explained by a large number of vacancies and an increased value of the isobaric-isothermal potential.

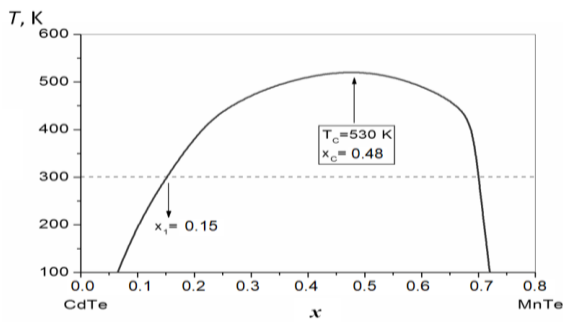


**Fig. 3.** Phase diagram of the  $\text{Cd}_{1-x}\text{Mn}_x\text{Te}$  solid solutions spinodal decomposition.

Information on stability of solid solutions can be obtained from the first principles calculations of the total energy [19]. However, these calculations are quite laborious, especially for irregular solid solutions, which are modeled using the supercells with a large number of atoms. It is also possible to study instability of solid solutions at the microscopic level on the basis of analyzing the charge density distribution of valence electrons, since the total energy is closely related to it.

An analysis of the charge density distribution by using the empirical pseudopotential method showed that stability of the solid solution is defined by the ratio of the destabilizing contribution of deformations associated with the lattice constant mismatch and the stabilizing charge exchange between different chemical bonds. It was proposed to use the degree of asymmetry of the spatial distribution of valence charge as a parameter that characterizes the ionicity of the bond [20]. Evolution of the charge density of upper valence bands, polarity, and transverse effective charge with changes in the solid solution composition can give a real picture of the influence of various alloying effects on the nature of chemical bond. The electron band structure of binary CdTe and MnTe was calculated using the empirical pseudopotential method in the plane wave basis with account of spin-orbit coupling. Solid solutions were modeled in the modified virtual crystal approximation.

The total charge density of the valence electrons  $\rho(\vec{r})$  was calculated by summation over Brillouin zone by using special points [21]:

$$\rho(\vec{r}) = 2e \sum_{n,\vec{k}}^{\text{OCC}} |\psi_{n,\vec{k}}(\vec{r})|^2, \quad (9)$$

where  $\psi_{n,\vec{k}}(\vec{r})$  is the electron wave functions obtained from the solution of secular equation,  $n$  is the zone number,  $\vec{k}$  is the wave vector. According to [20], the charge density can be separated into symmetric and asymmetric components:

$$\rho_S(\vec{r}) = \frac{1}{2} [\rho(\vec{r}) + \rho(-\vec{r})], \quad (10)$$

$$\rho_A(\vec{r}) = \frac{1}{2} [\rho(\vec{r}) - \rho(-\vec{r})]. \quad (11)$$

Expanding the density into the Fourier series

$$\rho(\vec{r}) = \sum_{\vec{G}} \rho(\vec{G}) e^{i\vec{G}\vec{r}}, \quad (12)$$

it is possible to determine the charge asymmetry coefficient in the following way:

$$g = \sqrt{\frac{S_A}{S_S}}, \quad (13)$$

where

$$S_S = \sum_{\vec{G}} |\rho_S(\vec{G})|^2 = \frac{1}{\Omega} \int_{\Omega} \rho_S^2(\vec{r}) d\vec{r}, \quad (14)$$

$$S_A = \sum_{\vec{G}} |\rho_A(\vec{G})|^2 = \frac{1}{\Omega} \int_{\Omega} \rho_A^2(\vec{r}) d\vec{r}, \quad (15)$$

where  $\Omega$  is the unit cell volume.

The charge density distribution  $\rho(\vec{r})$  of the CdTe and MnTe compounds is presented in Fig. 4. The maximum of the CdTe charge density is higher than that of MnTe and is closer to the anion, which indicates its higher degree of ionicity.

Theoretically, the process of solid solution formation in this approach can be separated into several stages. The first stage in modeling is fitting the binary compounds to the lattice constants of resulting solid solution, in this case, compression of CdTe and tension of MnTe take place. At the second stage, we combine MnTe and CdTe into a solid solution without relaxation of bond lengths and angles. Since the Mn–Te and Cd–Te bonds have different electronegativity, there will be a charge exchange between them. The charge is redistributed from the less ionic Mn–Te bond to the more ionic Cd–Te ones, which leads to a decrease in the difference in the charge distribution along with them. Relaxation of bond lengths at the last stage leads to displacement of atoms from the ideal positions specified by Vegard’s rule [22], and also causes redistribution of the charge on the bonds due to resulting deformations.

Thus, the joint impact of all the considered effects leads to smoothing the charge distribution along various bonds and approaching the real solid solution to the “virtual crystal” model. In the solid solution model, the strain fields due to the lattice distortion around substituted atoms pin the dislocations and thus slow down their motion. Therefore, formation of the solid solution is

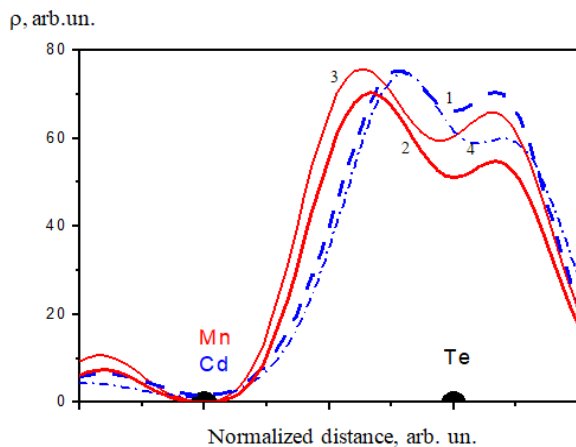


**Fig. 4.** Charge density distribution between different bonds during formation of the  $\text{Cd}_{1-x}\text{Mn}_x\text{Te}$  solid solutions: thick curves – in the CdTe (1) and MnTe (2) compounds; thin curves – in the  $\text{Cd}_{0.54}\text{Mn}_{0.46}\text{Te}$  solid solution; solid curves – along the Mn–Te bond (3); dashed curves – along the Cd–Te bond (4).

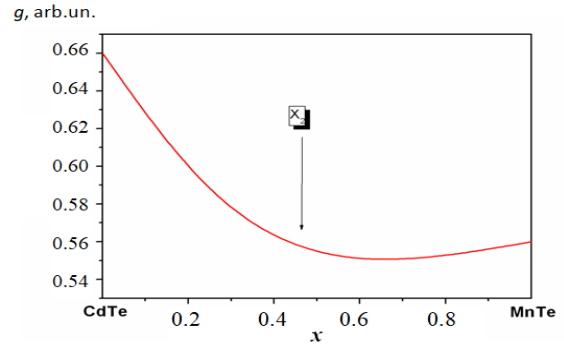


**Fig. 5.** Compositional dependence of the charge asymmetry coefficient  $g(x)$ :  $g(\text{MnTe}) = 0.56$ ,  $g(\text{CdTe}) = 0.66$ .

accompanied by the increase in the microhardness from 0.50 up to 0.67 GPa with an increase of  $x$  within the range 0..0.15. Spinodal decomposition that begins at  $x = 0.14$  leads to a violation of the macroscopic homogeneity of the solid solution and, as a consequence, to a decrease in the microhardness. The second maximum in the composition dependence  $H_V(x)$  can be explained by the change in the nature of the chemical bond near  $x = 0.46$ . The total change in the charge density along with the bond during the transition from the binary compound to the triple solid solution is shown in Fig. 5. Charge transfer from the strong to weak bond leads to the destabilization of the system, which explains the second maximum  $x_2$  on the composition dependence of the microhardness (Fig. 2).

In addition, the calculated asymmetry factor for the solid solution under study (Fig. 5) decreases monotonically to  $x_2 \approx 0.46$  with increasing Mn content. The further increase in concentration  $x$  leads to the nonmonotonic dependence of  $g(x)$ , which results in formation of the local minimum in the compositional dependence of the asymmetry factor. The change in the nature of the chemical bond in  $\text{Cd}_{1-x}\text{Mn}_x\text{Te}$  at  $x_2 \approx 0.46$  explains the nonmonotonic character of the microhardness dependence on  $x$  near the indicated manganese concentration.

#### 4. Conclusions

The experimentally obtained compositional dependence of the  $\text{Cd}_{1-x}\text{Mn}_x\text{Te}$  solid solutions ( $0.02 \leq x \leq 0.55$ ) microhardness is substantially nonmonotonic. The analysis of thermodynamic stability and redistribution of the charge density along various bonds in the solid solution enabled to clarify the processes leading to formation of the  $\text{Cd}_{1-x}\text{Mn}_x\text{Te}$  solid solutions. Two mechanisms have been considered, which made it possible to explain the maxima of the microhardness at  $x = 0.14$  and 0.46. It has been found that stability of the solid solution is defined not only by the difference in the lattice constants of binary CdTe and MnTe compounds but also by the charge exchange between bonds with different degrees of ionicity and the change in the nature of chemical bonds in  $\text{Cd}_{1-x}\text{Mn}_x\text{Te}$ .

## References

- Luan L., Lv H., Gao L., He Y., Zheng D. Preparation and properties of hemispherical CdMnTe nuclear radiation detectors. *Nucl. Instrum. Methods Phys. Res. B*. 2020. **471**. P. 42–47. <https://doi.org/10.1016/j.nimb.2020.03.018>.
- Ilchuk H., Zmiiiovskia E., Petrus R. *et al.* Optical properties of CdMnTe film: Experimental and theoretical aspects. *J. Nano-Electron. Phys.* 2020. **12**, No 1. P. 01027. [https://doi.org/10.21272/jnep.12\(1\).01027](https://doi.org/10.21272/jnep.12(1).01027).
- Egarievwe S.U., Lukosi E.D, James R.B., Roy U.N., and Derby J.J. Advances in CdMnTe Nuclear Radiation Detectors Development. *Proc. 2018 IEEE Nuclear Science Symposium and Medical Imaging Conf. (NSSMIC)*, 2018. P. 1–3. <https://doi.org/10.1109/NSSMIC.2018.8824694>.
- Tomashyk V., Feychuk P., Shcherbak L. *Ternary Alloys Based on II-VI Semiconductor Compounds*. CRC Press, 2013. <https://doi.org/10.1201/b15302>.
- Roy U.N., Okobiah O.K., Camarda G.S. *et al.* Growth and characterization of detector-grade CdMnTe by the vertical Bridgman technique. *AIP Adv.* 2018. **8**, No 10. P. 105012. <https://doi.org/10.1063/1.5040362>.
- Triboulet R., Didier G. Growth and characterization of Cd<sub>1-x</sub>Mn<sub>x</sub>Te and MnTe crystals; contribution to the CdTe-MnTe pseudo-binary phase diagram determination. *J. Cryst. Growth*. 1981. **52**, No 2. P. 614–618. [https://doi.org/10.1016/0022-0248\(81\)90350-X](https://doi.org/10.1016/0022-0248(81)90350-X).
- Triboulet R., Heurtel A., Rioux J. Twin-free (Cd,Mn)Te substrates. *J. Cryst. Growth*. 1990. **101**, No 1. P. 131–134. [https://doi.org/10.1016/0022-0248\(90\)90951-G](https://doi.org/10.1016/0022-0248(90)90951-G).
- Odin I.N., Chukichev M.V, and Rubina M.E. Phase diagram and luminescent properties of CdTe–MnTe solid solutions. *Inorganic Materials*. 2003. **39**, No 4. P. 345–348. <https://doi.org/10.1023/A:1023267430158>.
- Orujlu E.N., Aliev Z.S., Jafarov Y.I. *et al.* Thermodynamic study of manganese tellurides by the electromotive force method. *Condensed Matter and Interphases*. 2021. **23**, No 2. P. 273–281. <https://doi.org/10.17308/kcmf.2021.23/3438>.
- Glazov V.M. and Vigdorovich V.N. *Microhardness of Metals and Semiconductors*. New York, Springer-Verlag, 2012. <https://doi.org/10.1007/978-1-4684-8246-1>.
- Gorai S.K. Estimation of bulk modulus and microhardness of tetrahedral semiconductors. *J. Phys.: Conf. Ser.* 2012. **365**. P. 012013. <https://doi.org/10.1088/1742-6596/365/1/012013>.
- Stringfellow G.B. Epitaxial growth of metastable semiconductor alloys. *J. Cryst. Growth*. 2021. **564**. P. 126065. <https://doi.org/10.1016/j.jcrysgro.2021.126065>.
- Deibuk V.G., Dremlyuzhenko S.G., and Ostapov S.É. Thermodynamic stability of bulk and epitaxial CdHgTe, ZnHgTe, and MnHgTe alloys. *Semiconductors*. 2005. **39**, No 10. P. 1111–1116. <https://doi.org/10.1134/1.2085255>.
- Deibuk V.G. Thermodynamic stability of thin CdZnSb epitaxial films. *J. Thermoelectricity*. 2017. No 1. P. 50–59.
- Yuriychuk I.M., Fochuk P.M., Bolotnikov A.E., James R.B. Ab initio GGA+U investigations of the structural, electronic, and magnetic properties of Cd<sub>1-x</sub>Mn<sub>x</sub>Te alloy. *Proc. SPIE*. **11114**. 2019. *Hard X-Ray, Gamma-Ray, and Neutron Detector Physics*. P. 111141Q. <https://doi.org/10.1117/12.2529263>.
- Fistul' V.I. *Decomposition of Supersaturated Solid Solutions*. Moscow, Metallurgiya, 1977 (in Russian).
- Landau L.D. and Lifshitz E.M. *Theory of Elasticity, Course of Theoretical Physics*, Vol. 7. Elsevier, London, 2005.
- Debbarma M., Das S., Debnath B. *et al.* Density functional calculations of elastic and thermal properties of zinc-blende mercury–cadmium–chalcogenide ternary alloys. *Met. Mater. Int.* 2021. **27**. P. 3823–3838. <https://doi.org/10.1007/s12540-020-00778-7>.
- Garcia A., Cohen M.L. First-principles ionicity scales. I. Charge asymmetry in the solid state. *Phys. Rev. B*. 1993. **47**, No 8. P. 4215–4220. <https://doi.org/10.1103/PhysRevB.47.4215>.
- Chadi D.J., Cohen M.L. Special points in the Brillouin zone. *Phys. Rev. B*. 1973. **8**, No 12. P. 5747–5753. <https://doi.org/10.1103/PhysRevB.16.1746>.
- Yu P., Jiang B., Liu W., Shao T., Gao P. Research progress on postgrowth annealing of Cd<sub>1-x</sub>Mn<sub>x</sub>Te crystals. *Crystal Research and Technology*. 2022. Published online 20 February 2022. <https://doi.org/10.1002/crat.202200007>.
- Mycielski A., Wardak A., Kochanowska D. *et al.* CdTe-based crystals with Mg, Se, or Mn as materials for X and gamma ray detectors: Selected physical properties. *Progress in Crystal Growth and Characterization of Materials*. 2021. **67**, No 4. P. 100543. <https://doi.org/10.1016/j.pcrysgrow.2021.100543>.

## Authors' contributions

**Dremlyuzhenko K.S.:** formal analysis, investigation, resources, writing – original draft, visualization.

**Yuriychuk I.M.:** methodology, investigation, resources, validation, writing – review & editing.

**Zakharuk Z.I.:** methodology, software, formal analysis, writing – review & editing, visualization.

**Deibuk V.G.:** conceptualization, methodology, software, investigation, writing – original draft, writing – review & editing, project administration.

## Authors and CV



**Kseniia S. Dremluzhenko**, PhD student and junior researcher at the V. Lashkaryov Institute of Semiconductor Physics, National Academy of Sciences of Ukraine. K. Dremluzhenko received her education in chemistry at the Chernivtsi National University, Ukraine. Her research interests include the synthesis of nanoscale materials. In particular, the synthesis of cadmium telluride nanoparticles and the study of the doping of nanoparticles of semiconductor elements. E-mail: xeniadr@gmail.com, <https://orcid.org/0000-0001-7989-880X>



**Ivan M. Yuriychuk**, Associate Professor, Senior Researcher of Department of Electronics and Energy at the Yuriy Fedkovych Chernivtsi National University, defended PhD thesis in Physics and Mathematics (Semiconductor Physics) in 1991 at the Chernivtsi State University. Dr I. Yuriychuk is authored over

120 publications, 3 patents, 2 textbooks. The area of his scientific interests includes physics of nanoscale semiconductor structures and quantum computing. E-mail: i.yuriychuk@chnu.edu.ua, <https://orcid.org/0000-0001-6475-8337>



**Zinaida Z. Zakharuk**, Senior Researcher of Department of General Chemistry and Chemical Material Science at the Yuriy Fedkovych Chernivtsi National University, defended PhD thesis in Physics and Mathematics (Semiconductor Physics) in 1970 at the Chernivtsi State University. Dr Z. Zakharuk is authored over 150 publications and 15 patents. The area of her scientific interests includes semiconductor technology and physics of semiconductors. E-mail: z.zakharuk@chnu.edu.ua, <https://orcid.org/0000-0002-9333-9948>



**Vitaly G. Deibuk**, Professor of computer engineering at the Yuriy Fedkovych Chernivtsi National University. Prof. V. Deibuk received his education in theoretical physics at the Chernivtsi National University. He received his PhD (1984) and Doctor of Physics and Mathematics (2004) in semiconductor physics. In 2005 Prof. Deibuk was appointed professor of the Department of Computer Systems and Networks at the Faculty of Computer Science of the Chernivtsi National University. His research interests include the modeling of the physical properties of condensed systems, the design of reversible computer systems, the theory of multivalued circuits, and artificial intelligence methods. E-mail: v.deibuk@chnu.edu.ua, <https://orcid.org/0000-0002-1216-0031>

## Особливості мікротвердості та термодинамічна стійкість твердих розчинів $Cd_{1-x}Mn_xTe$

К.С. Дремлюженко, І.Н. Юрійчук, З.І. Захарук, В.Г. Дейбук

**Анотація.** Досліджено особливості плавлення та вирощування кристалів твердих розчинів  $Cd_{1-x}Mn_xTe$  ( $0.02 \leq x \leq 0.55$ ), а також залежність їх мікротвердості від складу. Експериментально виявлено локальні максимуми мікротвердості при  $x = 0.14$  та  $0.46$ . Розглянуто термодинаміку утворення  $Cd_{1-x}Mn_xTe$  у моделі дельта-параметра ґратки, а також побудовано фазову діаграму спінодального розпаду даних твердих розчинів. Методом емпіричного псевдопотенціалу проведено аналіз розподілу густини валентного заряду при формуванні  $Cd_{1-x}Mn_xTe$  та його впливу на перебудову хімічного зв'язку. Стабільність твердих розчинів визначається не лише різницею постійних ґратки бінарних сполук CdTe та MnTe, а й обміном заряду між зв'язками з різним ступенем іонності та зміною характеру хімічного зв'язку.

**Ключові слова:** мікротвердість, напівпровідник, твердий розчин, термодинамічна стійкість, спінодальний розпад.